An experimental protocol to measure the parameters affecting the compressive strength of CFRP with a fibre micro-buckling failure criterion

P.-Y. Mechin[a,b,*], V. Keryvin[a,**], J.-C. Grandidier[c], D. Glehen[b]

[a] *Univ. Bretagne Sud, UMR CNRS 6027, IRDL, F-56321 Lorient, France*
[b] *GSeaDesign, Structural Design Office, F-56100 Lorient, France*
[c] *ISAE-ENSMA, UPR CNRS 3346, PPrime, F-86360 Chasseneuil-du-Poitou, France*

Abstract

Understanding axial compressive failure mechanisms and estimating the related strength in continuous fibre composites is of paramount importance in the design of their parts. The mechanism at stake is the *micro-buckling instability* of fibres, which is contained by the matrix. In experimental measurements, compressive strength in bending is consistently higher than in axial compression. Indeed, the induced strain gradient provides an additional containment, namely *structural effect*. The characterisation of all geometrical and materials properties is usually lacking for models describing these combined mechanisms. A comprehensive experimental protocol is proposed in this paper to measure all the input parameters involved in a design oriented failure criterion. An epoxy matrix/high-modulus carbon fibre composite material illustrates this protocol. The influence of some key parameters, including the initial misalignment of the fibre, is discussed, thanks to additional experimental results.

Keywords: carbon fibres; thermosetting resin; strength; mechanical testing

1. Introduction

Carbon Fibre Reinforced Polymers (CFRP) are widely used in many engineering fields (aeronautics, offshore, renewable energies, marine industry...) and specific custom applications (racing cars, racing yachts...). They bring both high specific stiffness and strength. From an engineering point of view, composite parts undergo compressive stresses (compression or bending loadings). In the case of wings (mainsail wing or the wing of an aircraft), bending loads will induce tension on one side and compression on the other side. Masts of racing yachts undergo quasi pure compression loadings due to the base tuning (dock-tuning) to ensure a sufficient tension in cables. Based on the observation that compressive strengths are usually lower than tension ones [14], compressive failure should be considered carefully. Therefore, a proper estimation of compressive strength will allow for an efficient design of structures.

In terms of predictive modelling, several approaches have been suggested [29, 3, 10, 9, 7, 28, 17, 31]. The widely accepted scenario leading to failure consists in the displacement of the fibre constrained by the matrix stiffness (see Figure 1). Unidirectional plies (UDs) of a laminate exhibit an initial misalignment of fibres (ϕ_0) due to the manufacturing process. When the compressive stress on the UD (σ in Figure 1) increases, the misalignment of the fibre increases. (Actually the term fibre waviness is more appropriate but thie former term will be used throughout the paper.) The matrix contains the

*Present address: Dassault Systèmes, Catia Composites, F-78140 Velizy-Villacoublay, France
**Corresponding author
Email addresses: (P.-Y. Mechin), vincent.keryvin@univ-ubs.fr (V. Keryvin), (J.-C. Grandidier), (D. Glehen)

propensity of the fibre to buckle under this compressive loading, mainly *via* its elastic stiffness. When the stress increases, the matrix yields and exhibits plasticity, resulting in a lower stiffness than the elastic one, and buckling is made easier. The matrix undergoes a huge shearing which reaches its maximum at the location of the maximum misalignment along the fibre. Bending of the fibre occurs, generating a deformation gradient through the fibre's section. Different scenarios of failure can then occur: namely fibre breakage; matrix failure or interface debonding. It usually occurs in the fibre (locally in bending) for CFRP with a specific failure mechanism named kinking, detailed by Argon [3] or Budiansky and Fleck [9].

Early models used a specific relationship between the macroscopic compressive stress on the UD and local shearing of the matrix due to the misalignment of the fibre [3, 10, 9]. The difference between all these models lies in the way the shear behaviour of UD or its constituents is described: from pure elastic to elasto-plastic with or without hardening. Among recent contributions to this field [25], Pimenta *et al.* [28] proposed an analytical micro-mechanical model taking into account the misalignment of the fibre and an elasto-perfecly plastic matrix. Extension of this work was developed by Gutkin *et al.* [18] by establishing a failure envelop under both compression and in-plane shear. Since fibre buckling may initiate from the specimen free edge, where the fibre support is substantially reduced, Berbinau [8] considered the importance of estimating the through-thickness stresses and include their influence on the stability of the UDs, especially the inter-laminar shear stresses of neighbouring plies. He nevertheless concluded [7] that the effect of resin softening and fibre waviness were the most significant parameters.

In terms of measurement of compressive strength, direct methods of com-

pressive testing are usually difficult to carry out. Applying a pure compressive stress field without any stress raisers and preventing the buckling of the specimens is tricky and compression tests show a lot of variability [35, 33, 2]. As quoted in [20, chap. 5] by F.J. Matthews, *It is clear that whichever compression method is used, great care must be taken with specimen preparation, operator training and in the execution of the test.* Indirect and easier to carry out methods, such as bending, are alternatively employed [17]. They are also close to service use loadings in composites structures. However, significant differences were observed between the direct and indirect ways of testing [36]. Indeed higher compressive stresses may develop in bending as compared to the compressive strength measured in carefully carried out compression experiments [36]. A structural effect accounting for the strain gradient induced by bending was then introduced by Drapier *et al.* [13] and Gardin *et al.* [16]. Further evidence of this strain gradient effect was also observed by Wisnom and Atkinson in constrained buckling tests [34]. This structural effect takes into account both the effect of the deformation gradient and the influence of off-axis neighbouring plies in laminates. It indicates that the compressive failure depends on the laminate sequence (thickness of the successive UDs [1], stiffness of neighbouring plies [7]) and the deformation gradient.

A model accounting for the combined contributions of fibre micro-buckling [9] and the structural effect (stacking sequence, strain gradient) [13, 34, 16] was proposed to describe the mechanism of failure in compression under flexural loading [17]. This model is also analytical so that it can be used for the fast design loop of composite structures. It requires a number of parameters to properly estimate the compressive strength. With some few exceptions [24, 23], the necessary parameters for the reported compressive strength es-

timations are not measured or assessed in a comprehensive way. (Neither of them considers the structural effect.) This is the case for the latter model [17]. The purpose of this study is therefore to establish a clear and comprehensive experimental protocol to measure all the parameters involved in this latter model [17], being geometrical or material, required to use the design oriented failure criterion to estimate the compressive strength of UD.

The paper is organised as follows. We will first recall the salient features of this model. We will then establish an experimental protocol, able to measure all the necessary parameters of this latter model. A composite material composed of an epoxy matrix with high modulus carbon fibres will be used as an example. The measured parameters will then be used to estimate the compressive strength of such a CFRP. The experimental value of compressive strength on this material will be measured in parallel by performing bending tests. Eventually, the estimated and experimental values will be compared and the sensitivity of some key parameters on the estimation will be discussed.

2. A design oriented criterion for estimating the compressive strength of unidirectional plies by fibre micro-buckling accounting for a structural effect

2.1. Fibre micro-buckling

Budiansky and Fleck [9] modelled the non-linear shear behaviour of UD γ (shear strain) vs. τ (shearstress) by using a Ramberg-Osgood (RO) description:

$$\frac{\gamma}{\gamma^y_{UD}} = \frac{\tau}{\tau^y_{UD}} + \frac{3}{7} \times \left(\frac{\tau}{\tau^y_{UD}} \right)^{n_{UD}} \quad (1)$$

It involves three material parameters (γ^y_{UD}, G_{UD}, n_{UD}) or (γ^y_{UD}, τ^y_{UD}, n_{UD}). G_{UD} is the shear modulus of the composite, τ^y_{UD} is a nominal shear yield stress for which the secant modulus is reduced to 70% of its initial value G_{UD}. γ^y_{UD} is defined as the elastic strain at the shear stress τ^y_{UD} so that $\tau^y_{UD} = G_{UD} \times \gamma^y_{UD}$. The coefficient $\frac{3}{7}$ is specific to a choice made in [9] related to the definition of τ^y_{UD}.

The compressive strength, referred to as σ^{stab}_{UD}, and calculated using Budiansky and Fleck's model is defined as the maximum stress applied on UD before the instability of the fibre appears:

$$\sigma^{stab}_{UD} = \frac{G_{UD}}{1 + n_{UD}\left(\frac{3}{7}\right)^{\frac{1}{n_{UD}}}\left(\frac{\phi_0/\gamma^y_{UD}}{n_{UD}-1}\right)^{\left(\frac{n_{UD}-1}{n_{UD}}\right)}} \tag{2}$$

2.2. Structural effect

The structural effect results in the increase of UD failure compressive strain and stress with respect to σ^{stab}_{UD}. It is due to several mechanisms that do not take place at the UD mesoscopic scale but rather at a larger, macroscopic scale (laminate). Three factors are included in the structural effect, namely the deformation gradient through the thickness due to bending loadings, the thickness of UD and the stiffness of off-axis neighbouring plies.

Experimental observations on the structural effect have been experimentally detailed and compared by Grandidier *et al.* [17], ending with the proposal of an analytical model (Eq. (3)) taking into account both the micro-buckling mechanism [9] and the structural effect [16]. The estimated compressive strength is called critical, referred to as σ^{crit}_{UD}, is higher than σ^{stab}_{UD} and

defined by:

$$\sigma_{\mathrm{UD}}^{\mathrm{crit}} = \sigma_{\mathrm{UD}}^{\mathrm{stab}} + 2\, r_{gf} \frac{\pi}{e_b} \sqrt{\frac{E_m E_f}{1-\nu_m^2} V_f (1-V_f)} \tag{3}$$

where r_{gf} is the gyration radius of fibre ($\mathrm{r}_{gf} = \sqrt{\frac{I}{S}}$, with I the second moment of area of the fibre, and S the area of the fibre's cross section), E_m and ν_m are respectively the Young's modulus and the Poisson's ratio of the matrix, E_f the longitudinal elastic modulus of the fibre, V_f the volume fraction of fibres and e_b the characteristic thickness of UD involved in the instability mode (a fraction of the total thickness of UD), which is discussed below.

Let us start with the definition of a critical thickness, e_c. As an example, for a UD layer containing the neutral axis (see Figure 2 - a), only the part in compression is considered for critical thickness (e_c), while for a laminate with different ply orientations $[0_2, \pm 45, 0_2, \pm 45, 0_4]_S$ (see Figure 2 - b), e_c is equivalent to the thickness of the two outer UD plies subjected to pure compression (the deformation gradient is neglected for small thicknesses). For a monolithic UD stacking (only 0° plies), the instability mode is located near the free edge due to the deformation gradient. As it has been demonstrated by Drapier *et al.* [12], the modal shape of the plastic instability has an impact on critical values. In the case of UDs under bending only a reduced part of thickness is considered to contribute to compression failure due to the distribution of the strain. In order to easily approximate this effect, Grandidier *et al.* [17] proposed the characteristic thickness to be $\mathrm{e}_b = 0.4 \times \mathrm{e}_c$ which permits correlation with experimental results in similar configurations (see Ref. [17] for details). On the other hand, in case of a laminate where UD plies located near the edge are relatively thin, these latter plies bear a high compression

stress with a reduced gradient due to their low thickness. Consequently the modal shape of instability extends on all UDs thickness, and the characteristic thickness should be approximate by $e_b = e_c$ as proposed in [17].

2.3. Necessary parameters to identify

In order to use the model (3), a number of experiments is required. Most of them were briefly described and some parameters measured in [17, 12, 23], but never in a comprehensive way. A comprehensive experimental protocol including specific tests is required and described schematically in Figure 3. These tests involve:

- microstructural observations to measure the geometrical parameters:
  - optical microscopy (OM) to measure the ply thicknesses e_{ply} as well as e_c and e_b and also the fibre misalignment ϕ_0;
  - scanning electron microscopy (SEM) to measure the fibre volume fraction V_f and fibre diameter D_f.
- mechanical tests on the constituents (fibre and matrix) as well as on the composite (UD) to measure the material parameters:
  - elasto-plastic shear behaviour of the UD ply, described by a RO behaviour (γ^y_{UD}, G_{UD}, n_{UD});
  - elastic properties of the matrix (E_m, ν_m);
  - longitudinal elastic modulus of fibre E_f.

3. A comprehensive experimental protocol to measure all the model parameters

This section has two objectives. Firstly, to introduce the composite material we used as a example of our protocol. Secondly, to present the set of experiments carried out (see Figure 3) and the results obtained.

3.1. Materials

The present study is focused on high modulus carbon fibres (HR40 - Mitsubishi) for both 0° plies (UD) and off-axis plies, which are commonly used in racing yachts design.

The associated matrix is a low curing temperature ($\sim$ 110°C) epoxy resin system (for confidentiality reasons, the reference of the matrix is not provided). The pre-impregnated CFRP supplier was able to produce a block of matrix ($100\times100\times20$ mm^3). To ensure that the reticulation of the thermoset polymer is exactly the same at all locations in the block, quality control experiments were performed using Differential Scanning Calorimetry (DSC822, Mettler Toledo) to define the quality of reticulation. No differences between samples from the skin or the core of the matrix block were found. The question of a possible difference betwen *in situ* and *ex situ* properties of the matrix has been addressed by using a micromechanical numerical model (periodic boundary conditions) with the properties of both matrix and fibres (see § 3.3.2) and their volume fractions to simulate the shear response of a UD. Comparisons with experimental results (see § 3.3.3) were found very conclusive. They are not reported here for sake of clarity and space limitations.

As for the laminate, the following stacking sequence was used: [+45, 0_9, -45, 0_{11}, -45, 0_9, +45]. To ensure the highest quality of the composite,

compaction is carried out every three plies to reduce void content in composites. Due to this compaction, plies located on the mould side are more compacted than those located on the vacuum bag side. Therefore, the properties of composites on the mould side and the vacuum bag side are different. Coupons have been heated up in an autoclave according to standard curing cycle recommanded by manufacturer and pressure is set to 3 bars throughout the curing cycle.

3.2. Microstructure

The analysis of the microstructure allows one to measure the parameters related to the structural effect: the thickness of the UD plies, the volume fraction of fibres and the radius of these fibres. For the analysis of the fibre micro-buckling mechanism, the measurement of initial existing misalignment in the composite is also required.

3.2.1. Laminate or macroscopic scale

The side of the composite laminate is polished by means of standard grinding techniques. The thickness of each ply e_{ply} of the composite laminate is then measured by optical microscopy (OM, Leica MZ16) and digital image analysis (ImageJ software [30]). Close to the mould side, $e_{ply} = 292 \pm 2$ µm, and $e_{ply} = 300 \pm 3$ µm close to the vacuum bag side.

3.2.2. Sub-ply or microscopic analysis

SEM (Jeol JSM 6460 LV) allows measurement of both the volume fraction of fibres (V_f) and their associated diameters (D_f). The latter is needed to calculate the gyration radius (r_{gf}). By using a magnification of x500 and

an energy of $\sim$ 20 kV, SEM precise views of fibres, as seen in Figure 4, are possible.

The measurement of V_f and D_f is carried out by digital image analysis (ImageJ - [30]). However, other solutions exist to measure the volume fraction of fibres, such as the calcination method [38]. This latter method consists in heating the composite in order to burn-off the resin without affecting the fibres (glass fibres or carbon fibres). The difference in mass between the initial composite and the fibres alone at the end of the measurement makes it possible to identify the mass fraction of matrix then back calculate the volume fraction of fibres. This measurement gives an average value of V_f obtained on a large volume while SEM measurements are localised measurements on reduced surfaces raising the issue of the representativeness of the measurement (Figure 4). The results were equivalent between measurement by imaging and calcination method (for the volume fraction of fibres considered), giving $V_f = 54 \pm 2$ %.

3.2.3. Initial misalignment of fibres

Measuring the initial misalignment of fibres ϕ_0 is one of the key-points for estimating σ_{UD}^{stab}. Wisnom [37] estimated a loss of 50% in strength with a ϕ_0 of 3° with respect to a perfect alignment. Based on this literature, the most accurate value of the initial misalignment is required. The measurement of ϕ_0 is however difficult to make. Indeed, it is a measurement over a microscopic size width but over a length of several millimetres, so the length-to-width ratio is extremely large.

The distribution of fibre misalignment angle (ϕ_0) was measured using Yugartis' method [39]. The method consists in cutting samples through the

fibres with a specific angle. The cross sections of fibres are therefore elliptic. By properly polishing the cutting face, the dimensions (height and width) of the ellipses were measured (see Figure 5). The initial misalignment of the fibre was calculated as proposed in [39]. This method was used in the study of Lee and Soutis [26]. About 1000 or more ellipse lengths were measured for each face (mould or vacuum bagging). The angle distribution was then calculated and sorted into the class interval width at the angle of 0.5°. The distributions were found to be centered at an angle close to the cutting angle. They were then transformed and centered to zero as shown in Figure 6. The standard deviation for the mould and vacuum bagging faces were found to be 0.61° and 0.83°, respectively, in agreement with values reported in literature [26].

3.3. Mechanical tests

The model (Eq.(3)) requires measurement of the axial elastic modulus of the fibre E_f and both the Young's modulus E_m and the Poisson's ratio of the matrix, as well as the non-linear shear behaviour of the ply (UD).

3.3.1. Tensile test on matrix

Tensile tests were performed on the sole matrix, following ISO standard [22], to measure its elastic properties with a universal testing machine (Instron 5567, 10 kN load cell). The longitudinal and transverse strains were measured using a non-contacting 3D optical system (Aramis 5M, GOM, Germany). Two video cameras (8-bit gray levels, 2050x2448 pixels images at 2 Hz) recorded the motion of a random pattern spray painted on the sample surface, by means of a digital image correlation (DIC) technique. Five dog-bone samples (gauge length of 25x5x2 mm^3) were tested for reproducibility at 1

mm/min. Load-unload cycles were performed to ensure that the response of the material was elastic.

3.3.2. Tensile test on fibres

Tensile tests were performed on individual fibres following ASTM standard [4]. Fibres were extracted from uncooked pre-impregnated carbon plies and isolated from matrix with solvent (acetone). They were then attached on a paper frame to obtain a gauge length of 10 mm. The average apparent diameter was determined as previously detailed using SEM. The frame was clamped on a universal testing machine (MTS, 2 N load cell), and loaded at a constant crosshead-displacement rate of 1 mm/min up to fracture. Tests were performed on fifty fibres for reproducibility. The post-processing of the longitudinal modulus was performed taking into account the compliance of the loading frame.

Experimental results on the axial modulus of fibre ($E_f = 361 \pm 51$ GPa) are in good agreement with the datasheet's values (~ 390 GPa).

3.3.3. Tensile test on a ± 45° laminate: shear behaviour of UD

A central point in the use of the model (Eq.(3)) is a relevant identification of the non-linear behaviour of the UD under shear loading. Pure shear loading on a UD is not easy to perform as suggested in [5]. In such a test, the UD is subjected to local effects that modify the pure shear behaviour. An alternative way is to carry out tensile tests on a +/-45° stacking according to ISO standard [21] (in-plane shear tests). Such tests were performed using a universal testing machine (Instron 5567, 30 kN load cell). In such a laminate, a ply at +45° or at -45° undergoes a quasi-pure shear loading equivalent to what happens at the location of maximum misalignment under compression.

10 mm bi-axial strain gauges (Kyowa) were glued on coupons at 0° and 90° with respect to the tensile axis. Ten samples with the dimensions 250x25x2 mm^3 composed of 8 plies were tested for sake of reproducibility.

The shear stress is defined as $\tau_{UD} = \frac{F}{2bh}$ with F the applied load, b the width and h the thickness of the coupon. The shear strain is defined as $\gamma_{UD} = \epsilon_0 - \epsilon_{90}$, with ϵ_0 the strain given by the 0° strain gauge and ϵ_{90} the strain given by the 90° strain gauge. The resulting $\tau_{UD} - \gamma_{UD}$ graphs are plotted in Figure 7. They are highly reproducible and only a typical curve is represented. A non-linear regression to extract the RO parameters (Eq. (1)) is made for each sample, with a maximum shear strain $\gamma_{fit} = 2\%$ which is applied to all samples. This latter value is chosen since compressive failure occurs at lower values of shear strain. This fit is superimposed on the same Fig. 7. The resulting RO parameters (γ^y_{UD}, G_{UD}, n_{UD}) are shown in Table 1. Let us highlight that this RO fit is by no means a constitutive equation able to deal with plasticity or possible damage [15] but a convenient and simple way to describe the loading curve for subsequent use in Eq. (2).

Of all the information that can be extracted from this tensile test, it is also advantageous to measure the longitudinal modulus (E_{BB}) of the laminate (± 45°) for the subsequent calculation of the experimental compressive strength of UDs (see § 4.1). This is made by using straightforwardly the axial stress information as well as the 0° strain gauge, in the linear range of the response. E_{BB} was found to be 13.3 ± 0.4 GPa.

All the parameters measured are gathered in Tables 1 and 2.

4. Comparison between the engineering design tool evaluations with experimental results

4.1. Experimental determination of the compressive strength by a four-point bending test

Four-point bending tests were carried out according to ASTM standard [6] with a universal testing machine (Instron 5567, 30 kN load cell) with a distance of 90 mm between the upper rollers, where pure bending occurs. Polyethylene plates were put under the rollers to minimise stress concentrations. As detailed in Section 3.1, the following stacking sequence was used: [+45, 0_9, -45, 0_{11}, -45, 0_9, +45]. In any case discussions on the choice of the layup including ply orientation, ply thickness are out of the scope of the paper. A specific span (460 mm) was used for these high modulus fibres. Accordingly, the specimens had the following dimensions: 500x30x10 mm^3. Mono-axial strain gauges (10 mm in length - Kyowa) were glued on both the compressive side (strain ϵ_c^j) and the tension side (strain ϵ_t^j). Ten monolithic samples were tested. Five were broken with the mould side in compression, five with the vacuum bag side in compression. Failure occurred between the upper rollers. The force on the assembly and the two strain gauges signals were recorded during loading and synchronised. The force-displacement curves were all linear up to failure.

The Euler-Bernouilli kinematics assumption is considered valid, since the thickness of the specimen is small vis-à-vis its length. Therefore the deformation gradient through the thickness is constant. The position of the neutral plane (where the longitudinal strain is null) vis-à-vis the mid-plane (λ) is given by the two strain gauges at the top and the bottom of the specimens,

and computed as (4).

$$\lambda = -(\frac{h}{2} + e_g)\frac{\epsilon_c^j + \epsilon_t^j}{\epsilon_c^j - \epsilon_t^j} \tag{4}$$

where h and e_g are the thickness of the sample and the thickness of the glue between the sample and the strain gauge (taken $\sim$ 0.08 mm [1]). λ differs slightly from zero. It is always negative and is $\sim$ 0.1-0.2 mm. As quoted by Allix *et al.* [1], the origin is to be found in the asymmetry between the longitudinal tensile and compressive elastic behaviours. We follow the identification procedure of the compressive strength proposed by these authors by assuming that the tensile elastic modulus (E_{UD}^T) differs from the compressive one (E_{UD}^C) and that the latter parameter decreases linearly with the compressive strain (initial modulus E_{UD}^{C0} and slope α). We use their identification procedure of these three parameters by minimising simultaneously (for all measured points during loading) the gap between an estimated normal force and zero and an estimated bending moment and the measured one. We control the quality of the identification by calculating error indicators on the normal and the bending moment and making them very similar ($\sim$ 1‰). In doing this, we use the tensile moduli of the off-axis plies and the position of each block of plies of the same nature vis-à-vis the neutral plane λ. Values of E_{UD}^T, E_{UD}^{C0} and α were found to be 207 $\pm$ 3 GPa, 194 $\pm$ 3 and 13 $\pm$ 2 GPa/%, respectively.

The position of UD where the instability is assumed to take place is taken as the boundary between the topmost UD and the upper off-axis ply. Next, the strain at failure at this position is calculated as the deformation gradient (given by the two strain gauges and the thickness of the specimen) times the

position of the UD. Finally, the compressive strength $\sigma_{\text{UD}}^{\text{fail}}$ is calculated as the actual compression modulus times the strain at failure in UD. The mechanism responsible for failure was checked to be fibre microbuckling by observing the broken surfaces by OM (fibre kinking) and SEM (tensile and compressive fracture surfaces of broken fibres).

4.2. Estimation of compressive strength with the design oriented failure criterion

Using all the previously measured parameters in § 3, the compressive strength $\sigma_{\text{UD}}^{\text{crit}}$ was estimated combining the fibre micro-buckling contribution (Table 1) as well as the structural effect (Table 2). For the former, estimations were made assuming an initial misalignment ϕ_0 to be either one or two standard deviations of the fibre misalignment normal distribution.

5. Discussion

A comparison between the measured and estimated compressive strength of the UD is made in Table 3 and Figure 8. Let us recall that it is in no case a validation of the failure criterion relevance but rather a comparison on its use in an engineering context. Additional microstructural features such a void content, resin rich regions is beyond the scope of this paper.

The contribution of the micro-buckling effect (see Table 1) is the largest part of the compressive strength prediction. The structural part contributes to ~ 15 % of the compressive strength (with respect to the experimental values) for the stackings considered. As seen in Eq. (3), parameters r_{gf}, E_m, ν_m, E_f and V_f play in turn a minor role on the structural part. Therefore, information from suppliers datasheets is sufficient in terms of fibre diameter and volume fraction or materials elastic parameters. For instance the elastic asymetry

in compression w.r.t. to tension for the fibres or the matrix is not of high importance. The choice of the characteristic thickness e_b, as discussed in Section 2, has, at the contrary, an influence on the structural part.

From the experimental point of view, compressive failure on the mould side provides higher values than on the vacuum bag side (~ 15 %). According to the model, a different initial misalignment that increases the shear loading of the UD explains this difference. The analytical model looks relevant for quantifying the effect of initial misalignment on compressive strength. According to our measurements, there is only a 0.2° (s.d.) difference between the mould side and the vacuum bag side. This causes an equivalent gap of 20 % on the compressive strength. The model is highly sensitive to initial misalignment, which in turn, is actually highly sensitive to the manufacturing process. These observations are in good agreement with estimations from Ref. [19, 37, 32].

The micro-buckling part of the model is the one that is so dependent on ϕ_0. It decreases non linearly with ϕ_0. It reduces by ~ 500 MPa from 1 to 2° (see Fig. 8). With the comparison between experiments and the estimated strength being so dependent on the choice of ϕ_0, it is necessary to discuss the choice of a meaningful value or of a range of meaningful values. In most models, the initial misalignment is unfortunately taken as an adjustable or tested parameter to correlate compressive strength estimations with experiments [23, 37, 19, 17]. In several observations, the large numerical sensitivity to the initial misalignment has been experimentally compared on pultruded composites with small initial misalignment angle (misalignment is measured using X-ray scanning tomography) [11]. Creighton *et al.* [11] observed an increase in 25 % of the compressive strength by reducing the initial misalign-

ment from 1.0° to 0.7°. However, samples with a larger ϕ_0 also contained a larger void content volume fraction that will necessarily also affect the compressive strength of UDs. Therefore, it is somehow difficult to consider this result as a straight validation of the effect of misalignment on the compressive strength prediction. This would be indeed very relevant to mastering a manufacturing process able to control the value of ϕ_0 without inducing any kinds of other defects to test whether the experimental influence of ϕ_0 on the compressive strength would follow that of the model. The micro-buckling effect will affect predominantly the fibres that are the most misaligned. The fibre misalignment distribution follows a normal distribution (see Fig. 6). The value usually taken for ϕ_0 [26, 24] is one standard deviation of the normal distribution. It represents a coverage probability of 68 %, meaning that 32 % of the fibre population will contribute to the instability. Such a choice of ϕ_0 is plotted in Fig. 8. For both mould and vacuum bagging faces, the model largely over-predicts the experimental results, as already related in the literature [24]. Another choice is to consider that the instability will be triggered by a smaller population of more misaligned fibres. Taking a value of ϕ_0 corresponding to 2 s.d. of the distribution gives a coverage probability of $\sim$ 95 %. Such a choice is also plotted in Fig. 8. In that case, the comparison is much better between estimations and measurements. It means that $\sim$ 5 % of the most misaligned fibres will trigger the micro-buckling instability.

The robustness of the model was tested for some other parameters that were thought of being of some influence on the compressive strength estimation. The compressive strength (micro-buckling of the fibre, σ_{UD}^{stab}) depends linearly on the shear modulus of the UD (G_{UD}). A variation of 10 % of this modulus increases or decreases σ_{UD}^{stab} by $\sim$ 9 %. Its measurement is made

without too much uncertainty regarding the behaviour and is reproducible over a large number of samples. On the other hand, an appropriate value for the characteristic thickness (e_b) can be discussed depending on the deformation gradient effect. From an analytical point of view, a variation of 10 % in e_b induces an increase or decrease of σ_{UD}^{crit} by $\sim$ 1 %. Therefore, it is not necessary to pay further attention to the measurement of ply thickness, e_{ply}, at least for monolithic composite laminates [27].

6. Conclusion

The axial compressive strength of unidirectional plies is one of the key design parameters for composites in structural engineering. Several models have been developed to describe the specific mechanism of compressive failure. The one used in this study is a failure criterion based on the microbuckling of the fibre, controlled by the shear elasto-plastic behaviour of the matrix. An additional contribution concerns a structural effect linked to the beneficial effect of a strain gradient, for instance induced by a flexural loading. This criterion is design oriented so that it can be used for the fast design loop of composite structures.

This paper presented a comprehensive experimental protocol to measure all the necessary input parameters of the criterion, which was lacking. It is by no means a validation of this failure criterion. It allows for the measurement of geometrical parameters such as fibre volume fraction, fibre radius, thickness of the plies and initial fibre misalignment. It also permits experimentally determination of material parameters such as the non linear shear elasto-plastic behaviour of the ply, the elastic properties of the matrix and the elastic longitudinal modulus of the fibre. An epoxy matrix/high modu-

lus carbon fibre composite was used as a representative example of this very protocol.

The compressive strength was then estimated by means of the measurement of these parameters. A comparison between this estimation and experimental values obtained by four-points bending tests with the same composite material was then made. The estimation of the compressive strength was found to be highly sensitive to the initial misalignment of fibres in the ply, in relative accordance with experimental observations. The choice of a proper value of this initial fibre misalignment required by the model was discussed in view of the fibre misalignment distribution and the experimental values. In no case, this paramater was chosen as a fiting variable. Estimations and experiments are closely related when 2 standard deviations of the fibre misalignment distribution is made. It also suggests that 5 % of the most misaligned fibres trigger the instability.

Attention must therefore be paid on convenient and accurate ways to measure the initial misalignment and its influence on compressive strength, without introducing other manufacturing defects such as porosities, that could affect the shear behaviour of the ply.

Acknowledgements

The authors are grateful to C. Baley (IRDL - UBS) for encouraging discussions, to F. Portanguen, K. Henry, A. Jegat, A. Magueresse, M. Grabow (UBS) for experimental support. We are also grateful to CDK Technologies (Racing yacht builder, France), especially S. Digard who provided all composites coupons and supported this program. Undergraduate students A. Boyer and O. Chabaat (UBS) are also acknowledged for experimental help. Partial fund-

ing from French ANRT (#2012/1621) is finally acknowledged.

Data availibility

The raw/processed data required to reproduce these findings cannot be shared at this time due to legal or ethical reasons.

References

[1] Olivier Allix, Pierre Ladevèze, and E. Vittecoq. Modelling and identification of the mechanical behaviour of composite laminates in compression. *Compos. Sci. Technol.*, 51(1):35–42, jan 1994. ISSN 02663538. doi: 10.1016/0266-3538(94)90154-6. URL http://linkinghub.elsevier.com/retrieve/pii/0266353894901546.

[2] O Anthoine, J-C Grandidier, and L Daridon. Pure Compression Testing of Advanced Fibre Composites. *Compos. Sci. Technol.*, 58(5):735–740, 1998. doi: 10.1016/S0266-3538(97)00158-9.

[3] A.S. Argon. Treatise on Materials Science and Technology. In *Fract. Compos.*, chapter 4, page 345. Academy Press, New York, herman edition, 1972.

[4] ASTM D3379-75. Standard Test Method for Tensile Strength anf Young's Modulus for High Modulus Single-Filament Materials, 1998.

[5] ASTM D5379 / D5379M. Standard Test Method for Shear Properties of Composite Materials by the V-Notched Beam Method, 2012.

[6] ASTM-D6272. Standard Test Method for Flexural Properties of Unreinforced and Reinforced Plastics and Electrical Insulating Materials by Four-Point Bending. *Annu. B. ASTM Stand.*, 08:1–8, 2010. doi: 10.1520/D6272-10.1.

[7] P Berbinau, C Soutis, P Goutas, and P T Curtis. Effect of off-axis ply orientation on 0 degrees fibre microbuckling. *Compos. Part A Appl. Sci. Manuf.*, 30:1197–1207, 1999.

[8] Pierre Berbinau. *A study of compression loading of composites laminates*. PhD thesis, Oregon State University, 1997.

[9] B Budiansky and NA Fleck. Compressive failure of fibre composites. *J. Mech. Phys. solids*, 41(1):183–211, 1993.

[10] Bernard Budiansky. Micromechanics. *Comput. Struct.*, 16(1-4):3–12, jan 1983. ISSN 00457949. doi: 10.1016/0045-7949(83)90141-4. URL http://linkinghub.elsevier.com/retrieve/pii/0045794983901414.

[11] C. J. Creighton and T. W. Clyne. The compressive strength of highly-aligned carbon-fibre/epoxy composites produced by pultrusion. *Compos. Sci. Technol.*, 60(4):525–533, 2000. ISSN 02663538. doi: 10.1016/S0266-3538(99)00153-0.

[12] S Drapier, J.-C. Grandidier, and M Potier-Ferry. A structural approach of plastic microbuckling in long fibre composites: comparison with theoretical and experimental results. *Int. J. Solids Struct.*, 38(22-23):3877–3904, may 2001. ISSN 00207683. doi: 10.1016/S0020-7683(00)00247-X. URL http://linkinghub.elsevier.com/retrieve/pii/S002076830000247X.

[13] Sylvain Drapier, Catherine Gardin, Jean-Claude Grandidier, and Michel Potier-ferry. Structure effect and microbuckling. *Compos. Sci. Technol.*, 56(96):861–867, 1996.

[14] R R Effendi, J J Barrau, and D Guedra-Degeorges. Failure mechanism analysis under compression loading of unidirectional carbon/epoxy composites using micromechanical modelling. *Compos. Struct.*, 31:87–98, 1995. doi: 10.1016/0263-8223(94)00060-3.

[15] Nicolas Feld, Olivier Allix, Emmanuel Baranger, and Jean Mathieu Guimard. Micromechanical prediction of UD laminates behavior under combined compression up to failure: Influence of matrix degradation. *J. Compos. Mater.*, 45(22):2317–2333, 2011. ISSN 00219983. doi: 10.1177/0021998311401084.

[16] C Gardin, Jean-Claude Grandidier, and M Potier-Ferry. Homogenized models for the modelling of instability in long fibre media. *Rev. Mec. appliquée théorique*, 1(March): 171–203, 2002.

[17] J.-C. Grandidier, P. Casari, and C. Jochum. A fibre direction compressive failure criterion for long fibre laminates at ply scale, including stacking sequence and laminate thickness effects. *Compos. Struct.*, 94(12):3799–3806, dec 2012. ISSN 02638223. doi: 10.1016/j.compstruct.2012.06.013.

[18] R. Gutkin, S.T. Pinho, P. Robinson, and P.T. Curtis. Micro-mechanical modelling of shear-driven fibre compressive failure and of fibre kinking for failure envelope generation in CFRP laminates. *Compos. Sci. Technol.*, 70(8):1214–1222, aug 2010. ISSN

02663538. doi: 10.1016/j.compscitech.2010.03.009. URL http://linkinghub.elsevier.com/retrieve/pii/S0266353810001107.

[19] NL Hancox. The compression strength of unidirectional carbon fibre reinforced plastic. *J. Mater. Sci.*, 10:234–242, 1975. ISSN 0022-2461. doi: 10.1007/BF00540347. URL http://link.springer.com/article/10.1007/BF00540347.

[20] J M Hodgkinson. *Mechanical Testing of Advanced Fibre Composites*. CRC Press, Boca Raton, 2000.

[21] ISO 14129. Fibre-reinforced plastic composites. Determination of the in-plane shear stress/shear strain response, including the in-plane shear modulus and strength by the +/-45 degrees tension test method, 1998.

[22] ISO 527-2. Plastics - Determination of tensile properties - Part 2 Test conditions for moulding and extrusion plastics, 1996.

[23] P. M. Jelf and N. A. Fleck. The failure of composite tubes due to combined compression and torsion. *J. Mater. Sci.*, 29(11):3080–3084, 1994. ISSN 00222461. doi: 10.1007/BF01117623.

[24] A Jumahat, C Soutis, F R Jones, and A Hodzic. Fracture mechanisms and failure analysis of carbon fibre / toughened epoxy composites subjected to compressive loading. *Compos. Struct.*, 92(2):295–305, 2010. ISSN 0263-8223. doi: 10.1016/j.compstruct.2009.08.010. URL http://dx.doi.org/10.1016/j.compstruct.2009.08.010.

[25] F Laurin, N Carrere, and J Maire. Laminated composite structures subjected to compressive loading : A material and structural buckling analysis. *Compos. Struct.*, 80:172–182, 2007. doi: 10.1016/j.compstruct.2006.04.074.

[26] J Lee and C Soutis. Thickness effect on the compressive strength of T800 / 924C carbon fibre - epoxy laminates. *Compos. Part A Appl. Sci. Manuf.*, 36:213–227, 2005. doi: 10.1016/j.compositesa.2004.06.010.

[27] P-Y Mechin, V Keryvin, J-C Grandidier, and D Glehen. An Analytical Approach to Estimate the Compressive Strength of Carbon Fibre Reinforced Plastics. In *4th Int. Conf. Innov. High Perform. Sail. Yachts*, pages 183–191, Lorient, France, 2017.

[28] S. Pimenta, R. Gutkin, S.T. Pinho, and P. Robinson. A micromechanical model for kink-band formation: Part II - Analytical modelling. *Compos. Sci. Technol.*, 69(7-8):956–964, jun 2009. ISSN 02663538. doi: 10.1016/j.compscitech.2009.02.003. URL http:

//linkinghub.elsevier.com/retrieve/pii/S0266353809000529.

[29] B.W. Rosen. Mechanics of composite strengthening. In *Fiber Compos. Mater. Semin. Am. Soc. Met. Met. Park. Ohio*, page 39, Cleveland, Ohio, 1965. American Society of Metals.

[30] Caroline A Schneider, Wayne S Rasband, and Kevin W Eliceiri. NIH Image to ImageJ: 25 years of image analysis. *Nat. Methods*, 9(7):671–5, jul 2012. ISSN 1548-7105. URL http://www.ncbi.nlm.nih.gov/pubmed/22930834.

[31] C. Soutis. Compressive strength of composite laminates with an open hole: Effect of ply blocking. *J. Compos. Mater.*, 47(20-21):2503–2512, 2013. ISSN 0021-9983. doi: 10.1177/0021998312466122. URL http://jcm.sagepub.com/cgi/doi/10.1177/0021998312466122.

[32] C. Soutis and N.A. Fleck. Static Compression Failure of Carbon Fibre T800/924C Composite Plate with a Single Hole. *J. Compos. Mater.*, 24(5):536–558, may 1990. ISSN 0021-9983. doi: 10.1177/002199839002400505. URL http://jcm.sagepub.com/cgi/doi/10.1177/002199839002400505.

[33] W J G T'Hart, R Aoki, H Bookholt, P T Curtis, I Krober, N Marks, and P Sigety. Garteur compression behaviour of advanced CRFP. In *AGARD Rep. 785. Util. Adv. Compos. Mil. aircraft. 73rd Meet. AGARD Struct. Mater. panel held San Diego; 7th-11th October, 1991.*, pages 10(1)–10(6), 1991.

[34] M R Wisnom and J W Atkinson. Constrained buckling tests show increasing compressive strain to failure with increasing strain gradient. *Compos. Part A Appl. Sci. Manuf.*, 28A: 959–964, 1997.

[35] Michael R. Wisnom. The effect of specimen size on the bending strength of unidirectional carbon fibre-epoxy. *Compos. Struct.*, 18(1):47–63, 1991. ISSN 02638223. doi: 10.1016/0263-8223(91)90013-O.

[36] Michael R Wisnom. On the high compressive strains achieved in bending tests on unidirectional carbon-fibre / epoxy. *Compos. Sci. Technol.*, 43:229–235, 1992.

[37] M.R Wisnom. The effect of fibre misalignment on the compressive strength of unidirectional carbon fibre/epoxy. *Composites*, 21(5):403–407, sep 1990. ISSN 00104361. doi: 10.1016/0010-4361(90)90438-3. URL http://linkinghub.elsevier.com/retrieve/pii/0010436190904383.

[38] R Y Yee and T S Stephens. A TGA technique for determining graphite fiber con-

tent in epoxy composites. *Thermochim. Acat*, 272:191–199, 1996. doi: 10.1016/0040-6031(95)02606-1.

[39] S.W. Yurgartis. Measurement of small angle fiber misalignments in continuous fiber composites. *Compos. Sci. Technol.*, 30(4):279–293, jan 1987. ISSN 02663538. doi: 10.1016/0266-3538(87)90016-9. URL http://linkinghub.elsevier.com/retrieve/pii/0266353887900169.

Parameter	Value			Unit
G_{UD}	3.57	±	0.07	GPa
γ^{y}_{UD}	1.16	±	0.03	%
n_{UD}	7.3	±	0.6	-
ϕ_0 (s.d., mould side)	0.61			°
ϕ_0 (s.d., vacuum bag side)	0.83			°
σ^{stab}_{UD} (1 s.d., mould side)	1599	±	61	MPa
σ^{stab}_{UD} (1 s.d., vacuum bag side)	1369	±	53	MPa
σ^{stab}_{UD} (2 s.d., mould side)	1101	±	58	MPa
σ^{stab}_{UD} (2 s.d., vacuum bag side)	910	±	44	MPa

Table 1. *Experimental parameters for the micro-buckling contribution σ^{stab}_{UD}, see Eq. (2) for details. The non linear shear behaviour of UD is described by a RO fit (see (1)) with parameters G_{UD}, γ^{y}_{UD} and n_{UD}, obtained from a tensile test on a ±45° laminate. ϕ_0 is the initial misalignment on both sides of the composite, taken as the standard deviation (s.d.) of the fiber misalignment distribution using Yurgartis method.*

Paramter	Value			Unit
E_m	3.2	±	0.1	GPa
ν_m	0.400	±	0.005	-
E_f	361	±	51	GPa
V_f	54	±	2	%
D_f	6.07	±	0.27	µm
e_b	0.4x(9x0.30) = 1.08			mm
σ_{UD}^{stru}	163	±	10	MPa

Table 2. *Experimental parameters for the structural effect σ_{UD}^{stru}, see Eq. (3) for details. The fibre volume fraction (V_f) and diameter (D_f) are obtained by SEM and digital image analysis. The elastic properties (Young's modulus E_m, Poisson's ratio ν_m) of pure matrix, is obtained by tensile testing. The longitudinal elastic modulus of fibre (E_f), is obtained from fibre tensile tests.*

	σ_{UD}^{fail}	σ_{UD}^{crit} (1 s.d.)	σ_{UD}^{crit} (2 s.d.)	Unit
Mould side	1221 ± 101	1762 ± 71	1264 ± 68	MPa
Vacuum bag side	987 ± 115	1532 ± 63	1073 ± 54	MPa

Table 3. *Experimental compressive strength of UD, σ_{UD}^{fail} (obtained by means of a four-points bending test) compared to the critical compressive stress estimated σ_{UD}^{crit} for one or two standard deviations (s.d.) of the fibre misalignement distribution.*

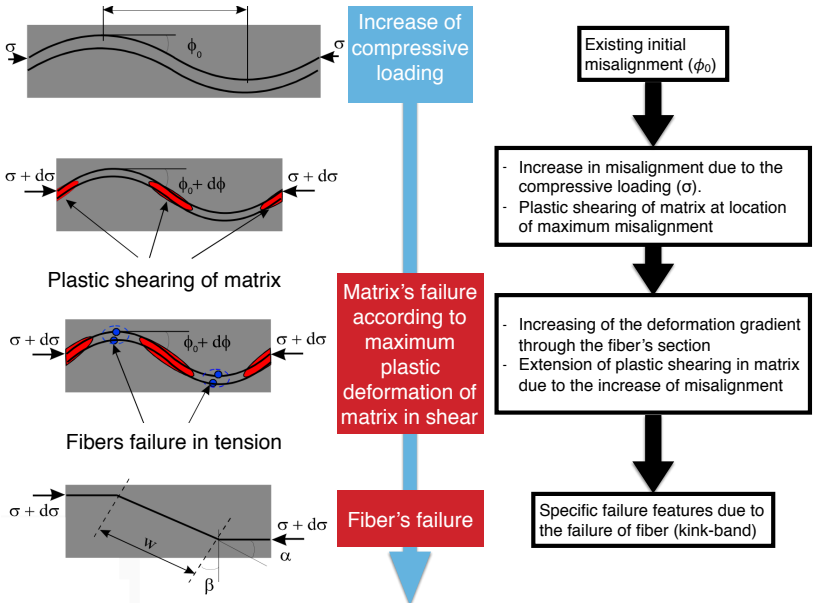

Figure 1. *Schematics of compression failure mechanisms leading to kinking band formation. The blue points correspond to the position of maximum axial stress through fibre's section (compression or tension) while the red surface is the area of the matrix exhibiting plasticity and extending due to the micro-buckling under compression.*

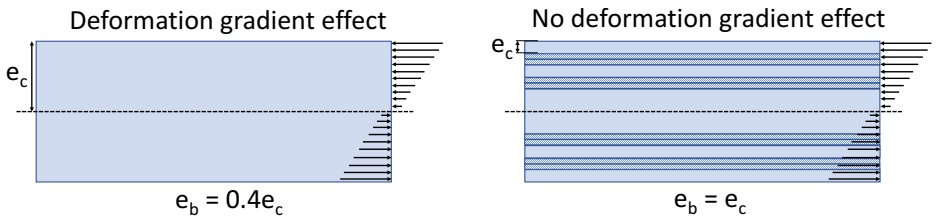

Figure 2. *Schematics for defining the critical thickness (e_c) and the characteristic thickness (e_b) involved in the structural effect (see Eq. (3)) and especially the case for the deformation gradient due to bending. Two examples are shown: (a) $[0]_{20}$ laminate, (b) $[0_2,\pm 45, 0_2, \pm 45, 0_4]_S$ laminate.*

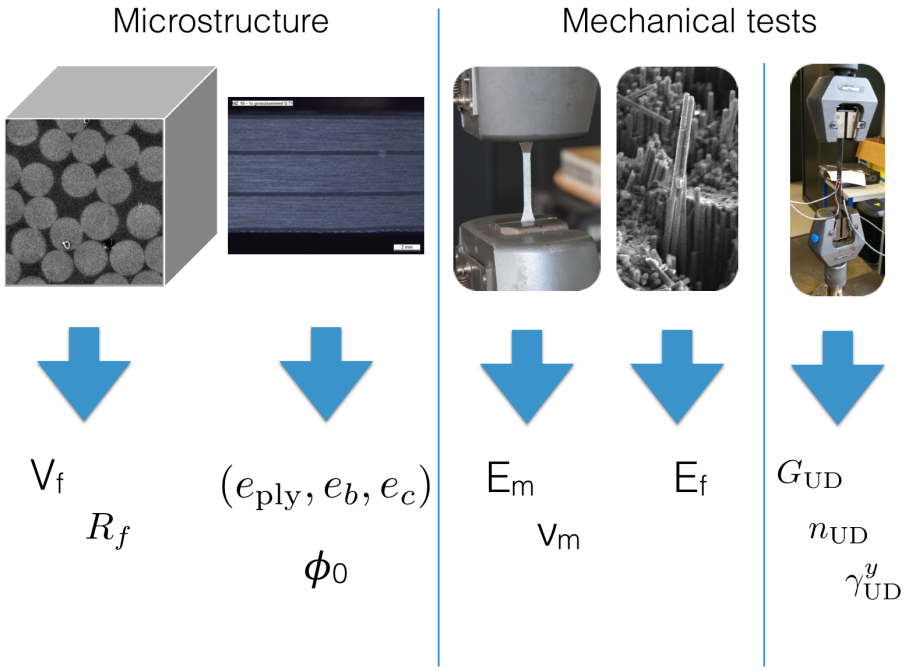

Figure 3. *Schematics of the experimental protocol proposed to measure all the parameters for the compressive strength model of Eq.* (3)

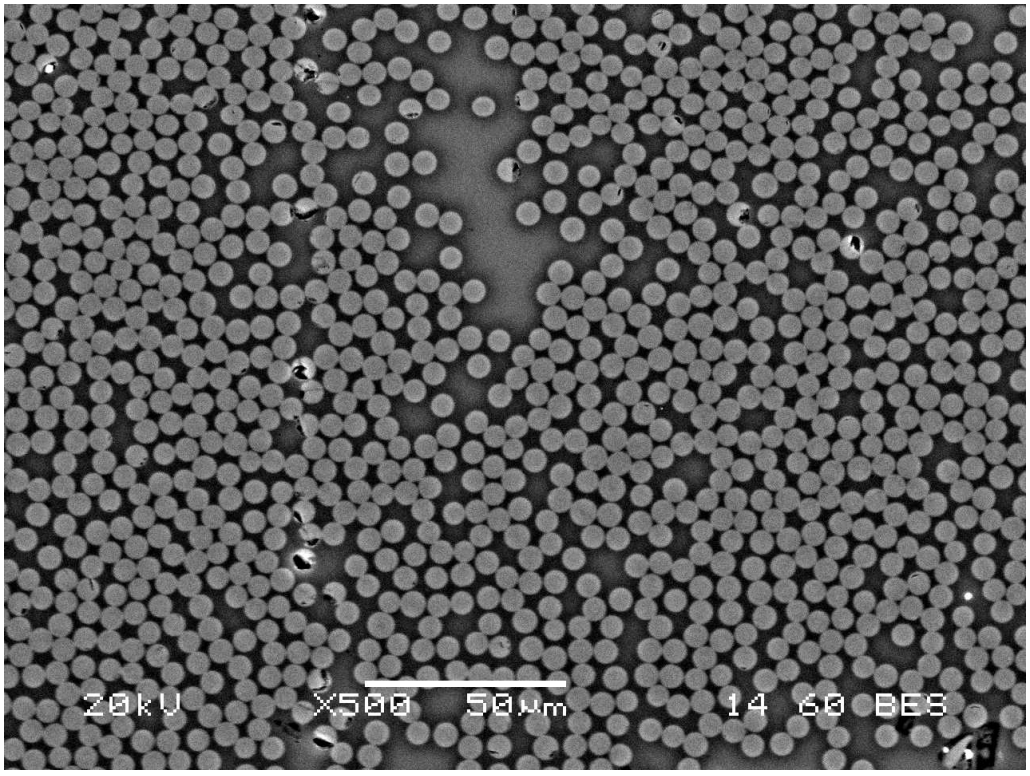

Figure 4. *SEM picture of a cross section of a 0° ply (UD) with unequal spatial distribution of the fibres in the matrix*

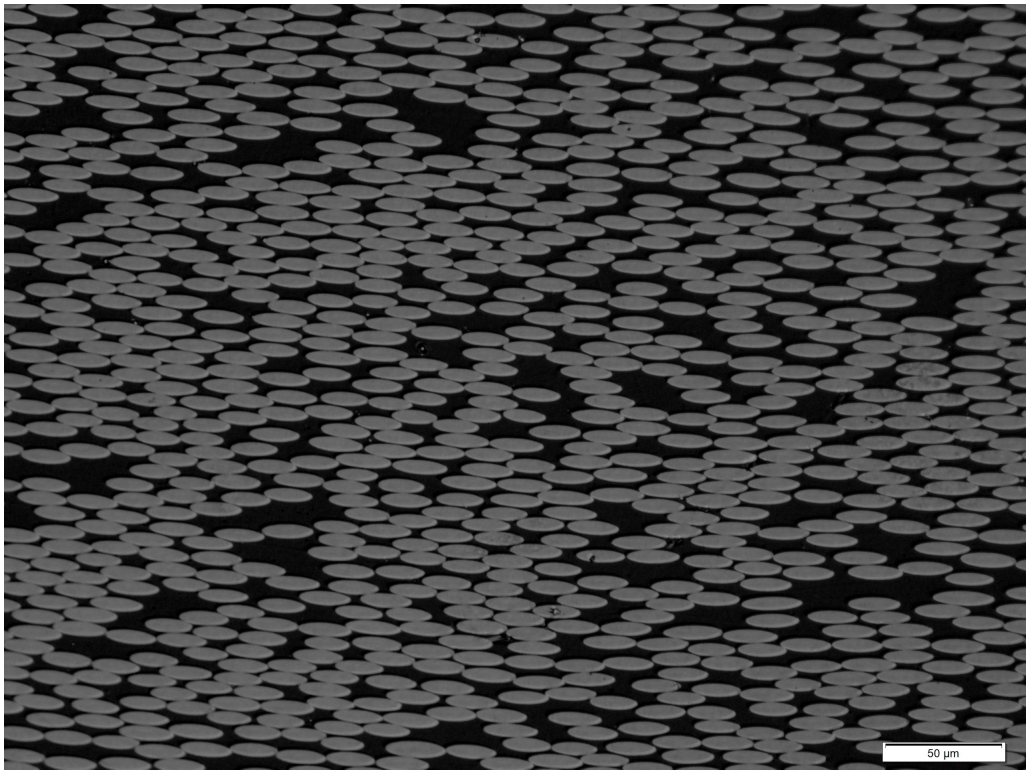

Figure 5. *OM picture showing the ellipses, formed by the fibres after cutting, used to obtain the fibre misalignement distribution using Yurgartis method*

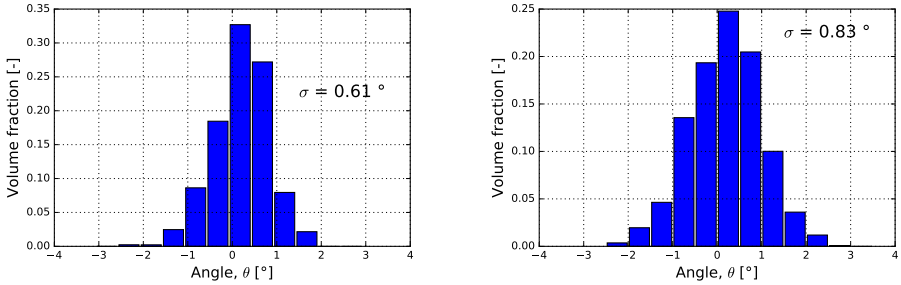

(a) (b)

Figure 6. *Fiber misalignment transformed distribution for the mould face (a) and the vacuum bagging face (b). The standard deviation (σ) is indicated.*

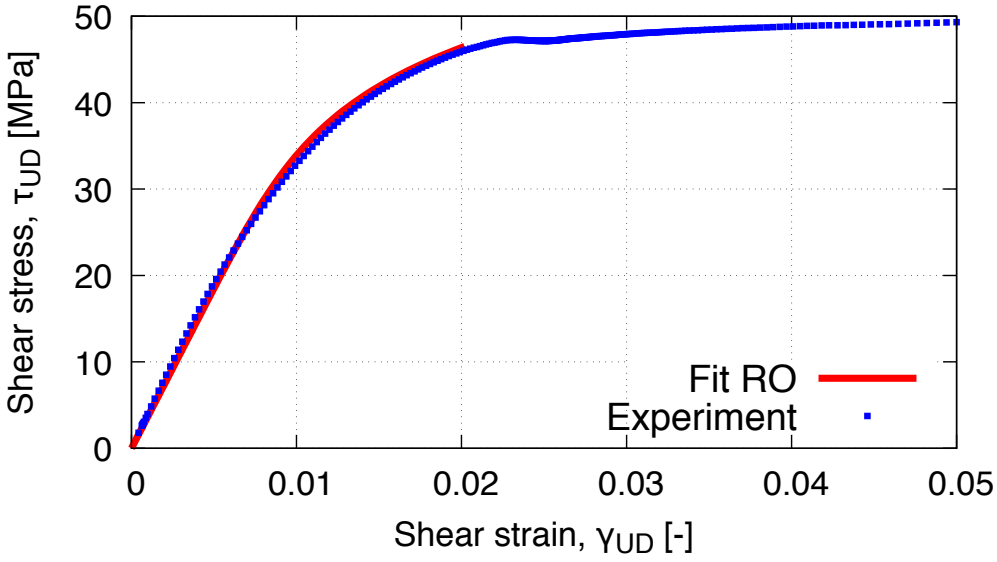

Figure 7. *Typical shear stress - shear strain curve of UD obtained from a tensile test on a ± 45° laminate. The plot range is restricted to 5% in shear strain but failure occurred much later. RO fits were made in the [0:2%] range in shear strain*

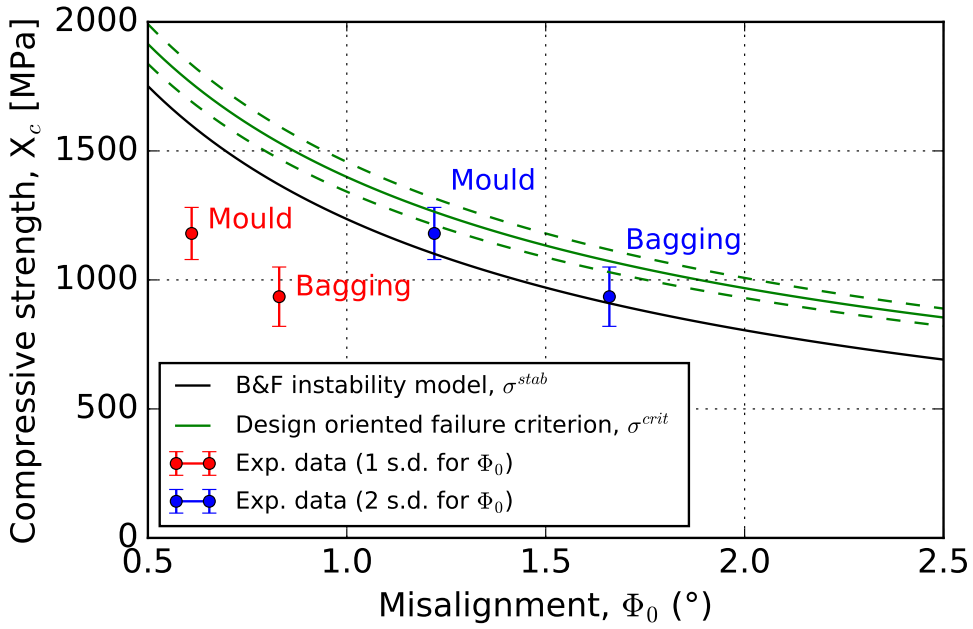

Figure 8. *Comparison of experimental and estimated values of the axial compressive strength of the epoxy matrix / high modulus carbon fibre composite material. Mould and vacuum bag sides are considered separately. The error bars come from the standard deviation of compressive strength for the experiments. Estimations of the Budiansky and Fleck micro-buckling model [9] and of the design oriented criterion are plotted. For the latter, the variations of the parameters (except ϕ_0) result in variations of the estimation (dotted lines).*